

# Hierarchical propagation of chirality through reversible polymerization: the cholesteric phase of DNA oligomers

Cristiano De Michele,<sup>\*,†</sup> Giuliano Zanchetta,<sup>‡</sup> Tommaso Bellini,<sup>‡</sup> Elisa Frezza,<sup>¶,§</sup>  
and Alberta Ferrarini<sup>¶</sup>

<sup>†</sup>*Dipartimento di Fisica, “Sapienza” Università di Roma, P.le A. Moro 2, 00185 Roma, Italy*

<sup>‡</sup>*Dipartimento di Biotecnologie Mediche e Medicina Traslazionale, Università di Milano, via F.lli Cervi 93, Segrate (MI) Italy.*

<sup>¶</sup>*Dipartimento di Scienze Chimiche, Università di Padova, via Marzolo 1, I-35131 Padova, Italy.*

<sup>§</sup>*present address: BMSSI, Uni. Lyon 1 / CNRS UMR 5086 CNRS, IBCP, 7 passage du Vercours, 69367 Lyon, France*

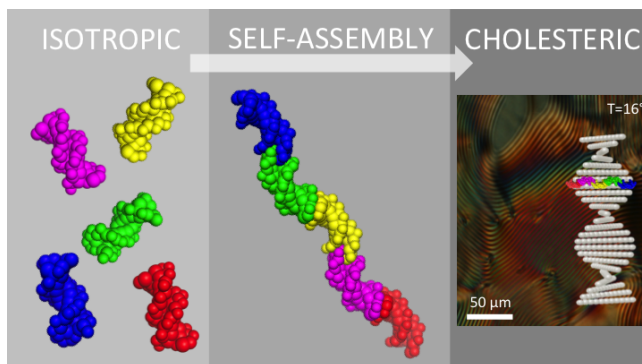
E-mail: cristiano.demichele@roma1.infn.it

## Abstract

Unveiling the subtle rules that control the build up of macroscopic chirality starting from chiral molecular elements is a challenge for theory and computations. In this context a remarkable phenomenon is the formation of helically twisted nematic (cholesteric) phases, with pitch in the micrometer range, driven by self-assembly of relatively small chiral species into supramolecular semi-flexible polymers. We have developed a theoretical framework to connect the cholesteric organization to the shape and chirality of the

constituents, described with molecular detail, in this kind of systems. The theory has been tested against new accurate measurements for solutions of short DNA duplexes. We show that the cholesteric organization is determined by steric repulsion between duplexes and we identify distinctive features of linear self-assembly in the temperature and concentration dependence of the pitch.

**for Table of Contents use only**



**Keywords:** cholesteric liquid crystals, reversible polymers, DNA, density functional theory, chirality propagation

When long range orientational order develops in concentrated solutions of rod-like chiral particles (lyotropic liquid crystal, LC), spontaneous breaking of the macroscopic chiral symmetry occurs, which is manifested as a helical rotation of the alignment axis. This characterizes the cholesteric ( $N^*$ ) phase, whose handedness and pitch depend on the structure of the constituent particles. However the relationship between these two levels remains far from being understood. This goal is made even harder by the variety of behaviors that have been reported.<sup>1-4</sup> The connection between microscopic and macroscopic chirality is a challenge also for theory and computations.<sup>5</sup> Theories developed for simple models have highlighted general features of the chirality propagation in lyotropic systems,<sup>6-17</sup> like the non straightforward relationship between particle and phase helicity. Nevertheless, the intrinsic complexity of systems that exhibit the  $N^*$  phase and the strong sensitivity of chirality propagation to details of the molecular structure and interactions prevent the assessment of theoretical pre-

dictions. Only in very few exceptions direct comparison between theoretical predictions and experimental data could be done.<sup>3,18–20</sup>

An important class of lyotropic liquid crystals is represented by self-assembling systems, where reversible aggregation introduces an higher level of complexity. In a series of experiments<sup>21</sup> it was shown that, above a critical concentration, 6 to 20 base long DNA duplexes (DNADs) order into the  $N^*$  phase with pitch on the micrometer scale.<sup>4,22</sup> This process is promoted by pairing and stacking interactions between the terminals of the DNADs that induce the formation of weakly bonded semi-flexible DNAD chains. Analogous propagation of chirality through hierarchical self-assembly is found in solutions of disc-like units like G-quadruplexes<sup>2</sup> or organic dyes and drugs<sup>23,24</sup> as well as of chiral disk-like micelles,<sup>25</sup> and has been proposed also for cellulose nanocrystals.<sup>26</sup> The inherent coupling between ordering and self-assembling makes it even harder to formulate a quantitative theory for the propagation of chirality in these systems.

In this letter, we propose a theoretical approach that relates the helical organization of self-assembly-driven  $N^*$  phases to the structure and chirality of the elementary building blocks. A benchmark for this approach is provided by solutions of the DNA Dickerson dodecamer (DD, sequence 5'-CGCGAATTCGCG-3'), which were found to form a right-handed  $N^*$  phase.<sup>4</sup> A preliminary study for monodisperse rigid systems of fixed lengths suggested that, somewhat unexpectedly for a polyelectrolyte, the cholesteric organization could be determined by the chirality of steric interactions between duplexes.<sup>27</sup> However, a definitive conclusion could not be drawn, since no quantitative comparison with experiments, nor analysis of temperature and concentration dependence of the pitch was possible, due to the lack of self-assembly in the theory. At the same time, theoretical studies on the untwisted  $N$  phase reached a deep understanding of the coupling between reversible physical polymerization and collective nematic ordering of DNADs<sup>28,29</sup> and of the effect of the oligomer structure on the formation of the LC phase.<sup>30</sup> Here we combine the molecular theory for  $N^*$  organization in systems where steric interactions dominate with that for self-assembly-driven nematic or-

der, thus making a significant step towards a realistic description of chirality propagation in lyotropic LCs.

We have performed new accurate and systematic measurements of the pitch of  $N^*$  phases of dense DD solutions. HPLC purified DD, purchased from Integrated DNA Technologies, was extensively dialyzed against a 10 mM NaCl solution and lyophilized. Dialysis proved critical to remove residual contamination, which is found to affect  $N^*$  properties and in particular the temperature dependence of the pitch. The new measurements here reported are thus not only more extended but also less affected by impurities than those of Ref.<sup>4</sup> The lyophilization step enables us to control the ionic strength through the NaCl/DNAD stoichiometric ratio, which was fixed to one NaCl molecule per ( $\text{Na}^+$ -neutralized) phosphate. Details on the measurement of  $N^*$  handedness and pitch are reported in the Supporting Information (SI).

Fig. 1-(a) shows the  $N^*$  pitch  $p$  measured as a function of temperature in samples of different concentrations. A right-handed  $N^*$  phase is formed ( $p > 0$ ), with a pitch of few microns. Lowering temperature and increase of concentration have the same effect of increasing the pitch (unwinding of the  $N^*$  helix). It may be noticed that the temperature dependence of the pitch obtained from the new measurements is different from that reported in ref.;<sup>4</sup> indeed, these measurements are very delicate, because the chiral behavior of the system is affected by even very small amounts of contaminants.

Our microscopic theory for  $N^*$  ordering builds on the general framework of classical density functional theory. A dominant role of steric repulsions is assumed and a second virial approximation is used, as in Onsager theory.<sup>31</sup> Theoretical and computational details can be found in the SI, here only a brief outline is given. The theoretical approach is based on the standard assumption that the orientational distribution function in  $N^*$  phase is identical to that of the untwisted N phase, which is justified by the large size of the  $N^*$  pitch compared to molecular length scale.<sup>6</sup> The Helmholtz free energy  $F$  of the  $N^*$  phase formed by a polydisperse mixture of self-assembling linear aggregates is expressed as a functional

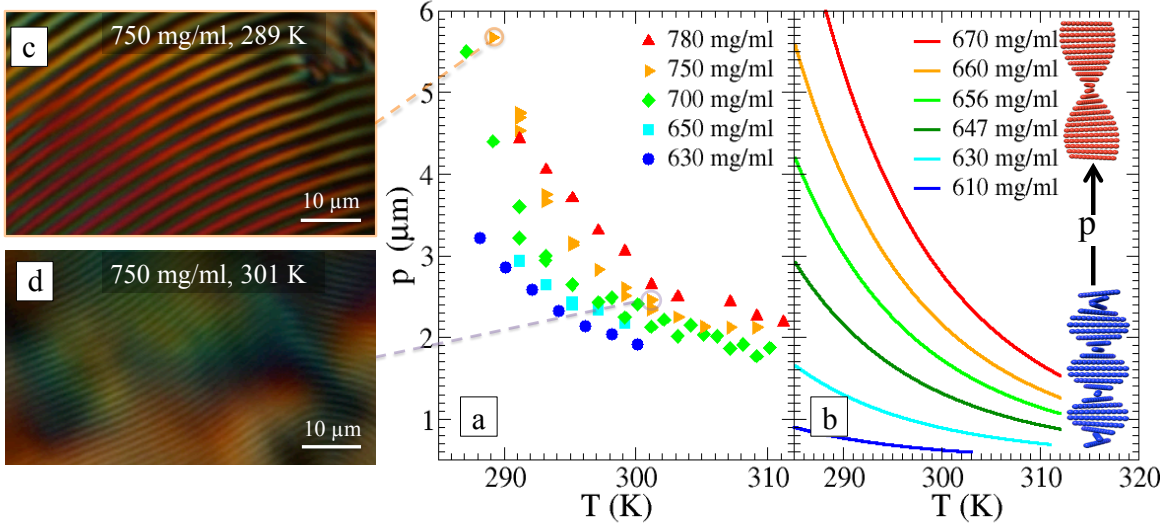


Figure 1:  $N^*$  pitch  $p$  in LC solutions of DD oligomers as a function of temperature along isochores, from experiments (a) and theory (b). Concentrations are given in the legend. (c) and (d) are  $N^*$  textures at different temperatures.

of the monomer density function,  $\bar{\rho}(l, \theta)$ . Here  $l$  is the length (or number of monomers) of the aggregate to which a monomer belongs and  $\theta$  is the angle between the long axis of the aggregate and the local LC director. The density function obeys the normalization condition  $\sum_l \int \bar{\rho}(l, \theta) 2\pi \sin \theta d\theta = \rho$ , where  $\rho = N/V$ , with  $N$  the number of monomers and  $V$  the volume, is the number density of monomers. We can write  $\bar{\rho}(l, \theta) = l\nu(l)f_l(\theta)$ , where  $\nu(l)$  is the number density of aggregates of length  $l$ , normalized such that  $\sum_l l\nu(l) = \rho$ , and  $f_l(\theta)$  is the orientational distribution function of aggregates of length  $l$ , normalized as  $\int f_l(\theta) 2\pi \sin \theta d\theta = 1$ . The Helmholtz free energy of the system can be written as the sum of the following contributions:

$$F = F^{id} + F^{excl} + F^{or} + F^{st} \quad (1)$$

where  $F^{id}$  is the ideal gas term and  $F^{or}$  describes the entropy decrease due to orientational order in the LC phase, and their form is well known (see SI).  $F^{excl}$  accounts for excluded volume interactions between aggregates and contains the information on the molecular structure.  $F^{excl}$  can be expressed as a function of the pitch  $p$ , or the corresponding wavenumber

$q = 2\pi/p$ , and for  $q \rightarrow 0$  can be approximated as:

$$\frac{F^{excl}}{V} = \frac{F_0^{excl}}{V} + qk_2 + \frac{q^2}{2}K_{22} \quad (2)$$

where  $F_0^{excl}$  is the contribution for the untwisted nematic phase,  $k_2$  is the chiral strength, which promotes the twist deformation, and  $K_{22}$  ( $>0$ ) is the twist elastic constant, which quantifies the force opposing such a deformation.  $k_2$  it is a signed pseudoscalar, which takes opposite values for enantiomers and determines the N\* handedness. The first term in Eq. (2) has the form:

$$\frac{F_0^{excl}}{V} = \frac{k_B T \eta(\phi)}{2} \sum_l \sum_{l'} \nu(l) \nu(l') \bar{v}_0^{excl}(l, l') \quad (3)$$

where  $\bar{v}_0^{excl}(l, l')$  is the mean of the mutual excluded volumes of aggregates of lengths  $l$  and  $l'$ , averaged over all their orientations, and  $\eta(\phi)$  is the Parsons-Lee factor, introduced to account for higher order terms in the virial expansion.<sup>32,33</sup> Analogous expressions can be written for  $k_2$  and  $K_{22}$ , where  $\bar{v}_0^{excl}(l, l')$  is replaced by  $\bar{v}_1^{excl}(l, l')$  and  $\bar{v}_2^{excl}(l, l')$ , respectively, the former depending on the chirality and the latter on the anisotropy of the excluded volume<sup>6,13</sup> (see SI for more details).

The last term in Eq. (1), i.e.  $F^{st}$ , accounts for stacking interactions and is expressed in terms of  $\Delta = \Delta(T)$ , the bonding free energy.<sup>34</sup> This term introduces into the free energy a nontrivial dependence on temperature, through the length distribution  $\nu(l)$ . At each value of the concentration  $c$  and temperature  $T$  the equilibrium state is determined by functional minimization of the free energy, Eq. (1), where only the first term in Eq. (2) is retained, with respect to the density function  $\bar{\rho}(l, \theta)$ . Thus, the length distribution  $\nu(l)$  and the orientational distribution function  $f(\theta)$  for the given thermodynamic conditions are determined. Finally, the equilibrium pitch is obtained by minimization of the free energy Eq. (2) with respect to the wavenumber  $q$ , which leads to  $p = -2\pi K_{22}/k_2$ . Calculations were performed as outlined in Ref.<sup>34</sup> For  $F^{st}$  the same functional form obtained in Ref.<sup>28</sup> was used and for the orientational distribution function the Onsager form was adopted,<sup>31</sup>

i.e.  $f_l(\theta) = (\alpha_N/4\pi \sinh \alpha_N) \cosh(\alpha_N \cos \theta)$ , where  $\alpha_N$  is a parameter that increases with the degree of orientational order. An exponential chain length distribution was assumed,  $\nu(l) = \rho M^{(l-1)}/(M-1)^{(l+1)}$ , with  $M$  the average chain length.<sup>34</sup>

A coarse-grained (CG) representation of DD aggregates was used,<sup>19</sup> generated from X-ray data<sup>35</sup> as explained in ref.<sup>27</sup> By employing this model we ensure that our theoretical approach takes properly into account all the relevant microscopic properties of the DD duplexes. The DD has a B-DNA conformation (right-handed) and in crystals it forms pseudo-continuous helices stabilized by end-to-end interactions, in which oligomers are staggered. CG models of DD and its aggregates are shown in Fig. 2 (b)).

The aggregate flexibility was introduced into the model in an effective way, through a characteristic length  $l_0$ , related to the persistence length  $l_p$ , which discriminates the regimes of stiff,  $l < l_0$ , and fully flexible chains,  $l \geq l_0$ , (see SI). By using the method proposed in Ref.,<sup>30</sup> we evaluated for the present DD model the persistence length  $l_p = 7.7$ , and in our calculations  $l_0 = 5$  was assumed, as determined in Ref.<sup>36</sup> for similar values of  $l_p$ .

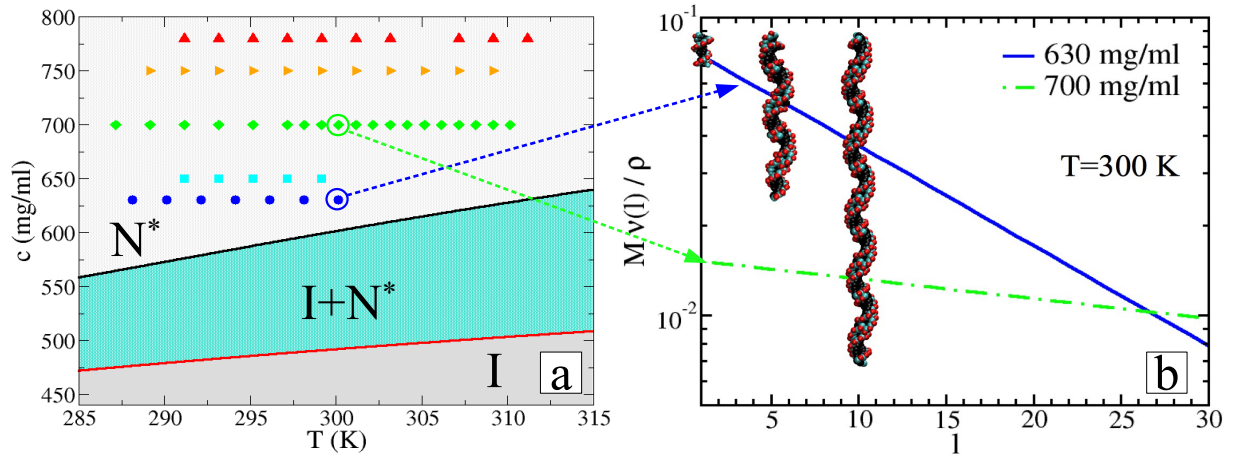


Figure 2: (a) Theoretical phase diagram of DD dodecamers. Symbols are experimental state points. (b) Normalized chain length distribution of DD aggregates,  $\nu(l)M/\rho$ , calculated at  $T = 300$  K for the concentrations  $c = 630$  mg/ml and  $c = 700$  mg/ml. The average chain length  $M$  is equal to 13.4 (630 mg/ml) and 66.0 (700 mg/ml). Superimposed to the plot: coarse-grained models of DD aggregates used in calculations.

Fig. 2 (a) shows the phase diagram calculated for DDs in the range of temperatures

and concentrations experimentally explored, where a transition from the isotropic to the cholesteric phase (I-N\* transition) can be observed. The plot in Fig. 2 (b) shows the normalized chain length distribution  $M\nu(l)/\rho$  obtained at two given state points, which, as a result of equilibrium polymerization, exhibits an exponential decay. The predicted distribution is quite broad and sensitive to the thermodynamic parameters. The average chain length  $M$  increases on increasing the concentration and on decreasing temperature, hence the I-N\* transition is shifted at higher concentration as temperature increases.

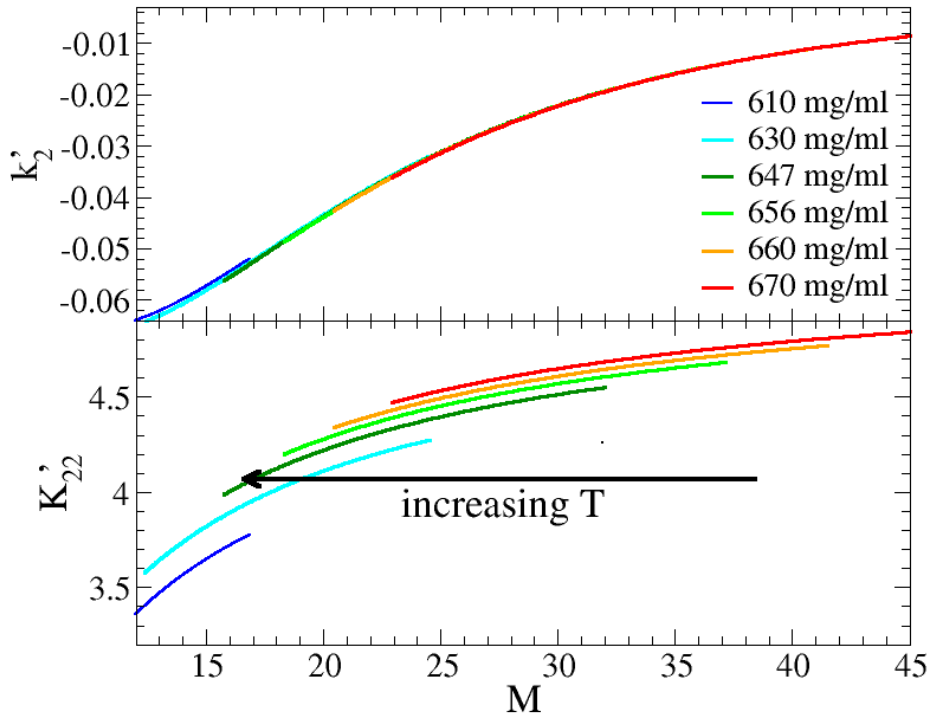


Figure 3: Reduced chiral strength  $k'_2$  and twist elastic constant  $K'_{22}$  calculated for solutions of DD at different concentrations, as a function of the average chain length  $M$ . For each concentration the  $M$  values corresponding to the temperature range considered in Fig. 1 are shown.

Fig. 1 (b) shows the N\* pitch, calculated as function of temperature for different concentrations. A right-handed N\* twist is predicted, in line with previous models of right-handed hard helical particles with tight pitch.<sup>6,13,14,27,37</sup> Both the magnitude of the N\* pitch and its dependence upon temperature and concentration are in agreement with experiment, although the effect of concentration is overestimated. Better agreement may require some improvement of the theory, in particular in what regards effects beyond the second virial and the

treatment of aggregate flexibility. It may be worth stressing that our theory contains no adjustable parameter other than those previously determined from the phase behavior, and that even the correct prediction of the N\* handedness is generally considered a success. Within our theory, the key factors are: the DD morphology, which determines the pitch handedness and the magnitude of the chiral strength  $k_2$ ; the functional form of the bonding free energy  $\Delta(T)$ , which controls the temperature dependence of the aggregate length distribution; the chain persistence length  $l_p$  and the related length  $l_0$ , which sets a limit to the effect of the increase in aggregate length on  $k_2$  and  $K_{22}$ . The magnitude of the pitch is rather sensitive to  $l_p$  and  $l_0$ . Indeed, it would increase by two orders of magnitude in the limiting case of very stiff aggregates.

The trend displayed in Fig. 1 is not heuristically obvious. Various behaviors have been reported in the literature for lyotropic N\* phases, but they remained generally unexplained. Here, by means of an adequate theoretical treatment, we can afford an insight into the underlying mechanism. To do so we introduce the dimensionless quantities  $k'_2 = k_2/D^4\eta(\phi)\rho^2k_B T$  and  $K'_{22} = K_{22}/D^5\eta(\phi)\rho^2k_B T$ , where a factor common to both terms, which thus do not affect the N\* pitch, have been removed. Fig. 3 shows  $k'_2$  and  $K'_{22}$  calculated for solutions of DD dodecamers, as a function of the average chain length  $M$ . In these plots each curve corresponds to a given concentration, where temperature increases on decreasing  $M$ . Along a curve  $K'_{22}$  increases as aggregates become longer, whereas  $|k'_2|$  decreases. This behavior can be readily understood considering that for stiff DD aggregates of average length  $M$ ,  $K'_{22} \sim (1 - 2M)^2$  and  $k'_2 \sim 1/M$ . The introduction of the length  $l_0$  sets a limit to the increase of  $K'_{22}$  and to the decrease of  $k'_2$ ; the effect is particularly strong for the former, which, in the  $M$  range under investigation, exhibits a change of about 20%, much smaller than the corresponding relative change of  $k'_2$ .

Within our theoretical modeling the temperature dependence of  $K'_{22}$  and  $k'_2$  is solely due to the self-assembly process, which is fully accounted for by the average chain length  $M$ . As temperature increases, at constant concentration,  $M$  decreases, and the results reported

in Fig. 3 show that  $K'_{22}$  decreases, whereas the magnitude of  $k'_2$  increases. Thus, both contribute to the tightening of the  $N^*$  pitch. In principle, the dependence of the pitch upon concentration is less straightforward,<sup>13,14</sup> since the effect of self-assembly is superimposed to the intrinsic influence of concentration on  $k'_2$  and  $K'_{22}$ , through the orientational order parameters. In Fig. 3 the effect of ordering results in differences between the curves at the same  $M$  value, which are small for  $K'_{22}$  and negligible for  $k'_2$ . Hence, the change in aggregate length distribution is also the main factor controlling the dependence of pitch upon concentration for DD.

We can now compare our results with experimental behaviors reported in the literature for other lyotropic cholesteric systems. For a number of other DNA oligomers, differing in length and sequence from DD, but all forming the  $N^*$  phase at very high concentration ( $>600$  mg/ml) a right-handed cholesteric twist was found, with temperature and concentration dependence analogous to those shown in Fig. 1.<sup>4</sup> However, for sequences exhibiting the  $N^*$  phase at lower concentration, as well as for long DNA, the opposite handedness (left) and temperature dependence of the  $N^*$  pitch was observed.<sup>1,4</sup> Such phenomenology has been ascribed to a competition between steric repulsions and electrostatic interactions in these systems.<sup>19,27</sup> Although in our work we actually consider only steric repulsion between duplexes, electrostatic interactions can be also taken into account as a next step, thus providing the opportunity to tackle this open and challenging issue. The  $N^*$  pitch behavior reported for several covalent polymers<sup>3,38</sup> is different from that shown in Fig. 1, but this is not inconsistent with the result of our theoretical analysis, according to which the temperature and density dependence of the pitch in DD solutions would be controlled by self-assembly.

In conclusion, we have developed a theoretical framework and a computational methodology that connects the helical structure of the  $N^*$  phase formed by reversible polymers to the structural features of the building blocks. Thus, we could afford a direct comparison with experimental data, which is beyond the capability of general theories for cholesteric order in lyotropic systems. DDs solutions turned out to be a suitable model system, because of

some beneficial features, which over-compensate its complexity: (i) the oligomer structure is known<sup>35</sup> and (ii) the N\* phase is formed at very high concentration (> 600 mg/ml) where an effective ionic strength well above 1 M ensures that electrostatic interactions are completely screened out. Therefore, high concentration, which has been ascribed to the bent shape of DDs,<sup>30</sup> is crucial for the dominant role of steric repulsion<sup>4,27</sup>

An analogy with DNA crystals can be seen, where helical packing based on simple geometric rules has been proposed to explain the common presence of stable right-handed crossovers, which correspond to helices mutually fitted by steric interactions in the major groove.<sup>39</sup> Our theoretical analysis confirms this picture and allows us to identify in the temperature and concentration dependence of the pitch an hallmark of self-assembly.

## Acknowledgement

We gratefully acknowledge support from PRIN-MIUR 2010-11 project (contract 2010LKE4CC). G.Z. acknowledges also support from the grant “*piano sviluppo unim2*”.

## Supporting Information Available

Experimental methods for the calculation of the cholesteric pitch. Detailed description of the theoretical approach and parameterization.

## References

- (1) Proni, G.; Gottarelli, G.; Mariani, P.; Spada, G. P. *Chem. Eur. J* **2000**, *6*, 3249–3253.
- (2) Bonazzi, S.; Capobianco, M.; De Morais, M. M.; Garbesi, A.; Gottarelli, G.; Ponzi Bossi, M. G.; Spada, G. P.; Tondelli, L. *J. Am. Chem. Soc.* **1991**, *113*, 5809–5816.

- (3) Sato, T.; Fato, Y.; Umemura, Y.; Teramoto, A.; Nagamura, Y.; Wagner, Y.; Weng, D.; Okamoto, Y.; Hatada, K.; Green, M. M. *Macromol.* **1993**, *26*, 4551–4559.
- (4) Zanchetta, G.; Giavazzi, F.; Nakata, M.; Buscaglia, M.; Cerbino, R.; Clark, N. A.; Bellini, T. *Proc. Natl. Acad. Sci. USA* **2010**, *107*, 17497–17502.
- (5) Frenkel, D., *Eur. Phys. J. Plus* **2013**, *128*, 10.
- (6) Straley, J. P. *Phys. Rev. A* **1976**, *14*, 1835–1841.
- (7) Odijk, T. *Macromolecules* **1986**, *19*, 2313–2329.
- (8) Osipov, M. A. *Nuovo Cimento D* **1988**, *10*, 1249–1262.
- (9) Emelyanenko, A. V. *Phys. Rev. E* **2003**, *67*, 1–25.
- (10) Wensink, H. H.; Jackson, G. *J. Chem. Phys.* **2009**, *130*, 234911:1–15.
- (11) Wensink, H. H.; Jackson, G. *J. Phys.: Condens. Matter* **2011**, *23*, 194107: 1–13.
- (12) Varga, S.; Jackson, G. *Mol. Phys.* **2011**, *109*, 1313–1330.
- (13) Frezza, E.; Ferrarini, A.; Kolli, H. B.; Giacometti, A.; Cinacchi, G. *PCCP* **2014**, *16*, 16225 – 16232.
- (14) Belli, S.; Dussi, S.; Dijkstra, M.; van Roij, R. *Phys. Rev. E* **2014**, *90*, 020503.
- (15) Wensink, H. H. *Europhys. Lett.* **2014**, *107*, 36001.
- (16) Grason, G. M. *ACS Macro Letters* **2015**, *4*, 526–532.
- (17) Zhao, W.; Russell, T. P.; Grason, G. M. *Phys. Rev. Lett.* **2013**, *110*, 058301.
- (18) Sato, T.; Nakamura, J.; Teramoto, A.; Green, M. M. *Macromol.* **1998**, *31*, 1398–1405.
- (19) Tombolato, F.; Ferrarini, A. *J. Chem. Phys.* **2005**, *122*, 054908.

- (20) Tombolato, F.; Ferrarini, A.; Grelet, E. *Phys. Rev. Lett.* **2006**, *96*, 258302.
- (21) Nakata, M.; Zanchetta, G.; Chapman, B. D.; Jones, C. D.; Cross, J. O.; Pindak, R.; Bellini, T.; Clark, N. A. *Science* **2007**, *318*, 1276–1279.
- (22) Rossi, M.; Zanchetta, G.; Klussmann, S.; Clark, N. A.; Bellini, T. *Phys. Rev. Lett.* **2013**, *110*, 107801.
- (23) Lydon, J. *J. Mater. Chem.* **2010**, *20*, 10071–10099.
- (24) Yang, S.; Wang, B.; Cui, D.; Kerwood, D.; Wilkens, S.; Han, J.; Luk, Y.-Y. *J. Phys. Chem. B* **2013**, *117*, 7133–7143.
- (25) Dörfler, H.-D. *Adv. Colloid Interface Sci.* **2002**, *98*, 285 – 340.
- (26) Lagerwall, J. P.; Schutz, C.; Salajkova, M.; J. Noh, J.; Park, J. H.; Scalia, G.; Bergstrom, L. *NPG Asia Mater.* **2014**, *6*, e80–.
- (27) Frezza, E.; Tombolato, F.; Ferrarini, A. *Soft Matter* **2011**, *7*, 9291–9296.
- (28) De Michele, C.; Rovigatti, L.; Bellini, T.; Sciortino, F. *Soft Matter* **2012**, *8*, 8388–8398.
- (29) Kouriabova, T.; Betterton, M.; Glaser, M. *J. Mat. Chem.* **2010**, *20*, 10366–10383.
- (30) Nguyen, K. T.; Battisti, A.; Ancora, D.; Sciortino, F.; De Michele, C. *Soft Matter* **2015**, *11*, 2934–2944.
- (31) Onsager, L. *Ann. N.Y. Acad. Sci.* **1949**, *51*, 627–659.
- (32) Parsons, J. D. *Phys. Rev. A* **1979**, *19*, 1225.
- (33) Lee, S. *J. Chem. Phys.* **1988**, *89*, 7036.
- (34) De Michele, C.; Bellini, T.; Sciortino, F. *Macromolecules* **2012**, *45*, 1090–1106.
- (35) Wing, R.; Drew, H.; Takano, T.; Broka, C.; Tanaka, S.; Itakura, K.; Dickerson, R. *Nature (London)* **1980**, *287*, 755–758.

- (36) Nguyen, K. T.; Sciortino, F.; De Michele, C. *Langmuir* **2014**, *30*, 4814–4819.
- (37) Harris, A. B.; Kamien, R. D.; ; Lubensky, T. C. *Mol. Phys.* **1999**, *71*, 1745–1757.
- (38) Dupre, D. B.; Duke, R. W. *J. Chem. Phys.* **1975**, *63*, 143–148.
- (39) Timsit, Y.; Moras, D. *EMBO J.* **1994**, *13*, 2737–2746.